Design and Implement of Step-Up DC-DC Converter with a Professional Approach using MATLAB/Simulink

Ali M. Jasim

Network Engineering Department, Al-Iraqia University, Iraq
Email:drali7819@gmail.com
https://orcid.org/0000-00002-3164-4410

Abstract

Step-up converters find extensive application in various sectors, including powered vehicles, photovoltaic systems, continuous power supplies, and fuel cell systems. This paper describes the process of designing and building a resistive load step-up (boost) converter, which is a widely used industry application for increasing the direct current (DC) input voltage. This study focuses on ascertaining the appropriate values for the inductor and capacitor within the circuit. The design primarily emphasizes continuous mode operation, involving varying voltage inputs of 10V and 20V DC, while employing a switching frequency input of 25 kHz with the IGBT serving as the switching device. The design evaluation of this circuit aims to regulate the input voltage to support a stable output voltage of 30 VDC, with a simulation power conversion efficiency of 96.18 percent for the input voltage,10V, and a simulation power conversion efficiency of 96.08 percent for the input voltage,20V. This examination also incorporates the requirement of a ripple inductor current, which should not exceed 25% of the total inductor current, and an output voltage ripple is less than 1%. The circuit design parameters are determined based on factors such as output voltage, inductor voltage, and inductor current waveform. MATLAB Simulink software will be used to check the circuit design, thus confirming the agreement between simulation results and theoretical predictions. The simulation results provide compelling evidence that the established model proficiently maintains the output voltage under diverse input voltage scenarios. As a result, these parameters are suitable for the construction of a fully operational boost converter circuit. This paper systematically presents all objectives, calculations, experiments, data, and results in a comprehensive manner.

Keywords- Step-up Converter, Input Voltage Source, Output Voltage Source, MATLAB/Simulink.

I. INTRODUCTION

In numerous industrial applications, there is a need to convert a DC input voltage into a variable DC output voltage. This process of directly converting DC voltage from one level to another is called a DC converter. Such converters are employed to elevate the input voltage to reach the desired level [1][2]. Each electronic circuit is presumed to function based on a supply voltage, typically considered as a constant. A voltage regulator is an electronic circuit within the field of power electronics. A power electronic circuit engineered to maintain a stable output voltage, regardless of variations in load current or line voltage. Various voltage regulators employing diverse control schemes are utilized, and as circuit complexity rises alongside technological advancements, there is an increasing demand for precise and swift regulation [3][4]. This has prompted the necessity for the development of more advanced and dependable designs for DC-DC converters. The DC-DC converter accepts an unregulated DC voltage input and produces a constant or regulated output voltage. The regulators can be primarily categorized as linear and switching regulators [5]. Each regulator incorporates a power transfer stage and control circuitry, responsible for monitoring the output voltage and adjusting the power transfer stage to sustain a consistent output voltage. DC/DC converters play a crucial role as integral components in renewable power conversion systems, serving as electronic operating systems for various power applications [6][7]. The majority of renewable sources, including photovoltaic (PV) systems and wind energy, typically generate a low voltage output. To meet the requisite voltage levels at the output, booster circuits are required. DC converters find extensive utilization in industrial scenarios, encompassing electric vehicle motor control, uninterruptible power supplies, and battery-powered devices [8].

They offer exceptional efficiency, precise acceleration management, and rapid dynamic responsiveness, making them suitable for the implementation of regenerative braking in DC motors to facilitate energy recovery into the power source. Typically, boost converters elevate the input DC voltage, drawing power from sources like batteries, solar panels, rectifier outputs, and DC generators. The operational control of the boost converter, as described [9][10] in depends on the duration of the switching process. This duration's ratio to the total switching time period is termed the switching duty cycle, denoted as D, as described by. The investigation primarily centers on continuous current mode operation, which, in this analysis, is denoted as the continuous positive cycle throughout the switching process [11][12]. The adoption of continuous current mode operation in this study is aimed at achieving enhanced regulation within the circuit. Predominantly utilized converters in power electronics encompass buck [13-16], boost [17-20] and buck-boost [21-24] converters. Nonetheless, in PV-based applications, the boost converter is the more prevalent choice, and this research proposal centers on a boost converter due to its superior stability and efficiency. The DC-DC converter, in conjunction with maximum power point tracking (MPPT) serves various other purposes as well. This characteristic leads to energy conservation in transportation

systems characterized by frequent changes in operational states. DC converters find utility in the realm of DC voltage regulation, and they are additionally employed, often in conjunction with an inductor, to establish a dedicated DC current source, particularly for applications such as the current source inverter. Switching power converters offer several primary advantages over linear converters, namely, enhanced efficiency, reduced physical footprint, and lower cost. Switching power converters typically exhibit efficiencies ranging from 70% to 80%, a significant improvement compared to the standard 30% efficiency typically associated with linear converters [27][28]. The inherent nonlinearity of DC-DC converters arises from the operation of the switching devices. As a consequence of these undesired nonlinear traits, the converters necessitate a controller with a heightened level of dynamic responsiveness. The Switching Boost Converter has been engineered to offer an effective means of elevating a provided DC voltage source to achieve a specific desired voltage level. In several aspects, a DC-DC converter serves as the DC counterpart to a transformer [29][30]. Primarily, the DC-DC converter comprises power semiconductor devices functioning as electronic switches, falling under the classification of switched-mode DC-DC converters. Among the various switching control methods, Pulse Width Modulation (PWM) is the most commonly employed. In DC-DC voltage regulators, maintaining a stable output voltage is of paramount importance, irrespective of fluctuations in the input voltage [31][32].

II. Step-up (Boost) Converter Circuit Operation

The fundamental circuit diagram of the operational boost converter is depicted in Figure 1. An inductor is incorporated to ensure a stable input current, with minor ripple components present in the input current. An inductor is incorporated to ensure a stable input current, with minor ripple components present in the input current [33][34]. Regarding voltage and current relationships, the analysis presupposes the presence of steady-state conditions. The switching period is denoted as "T," with the switch closed for a duration of "DT" and open for "(1-D)T". Under these conditions, the inductor current remains continuous, maintaining a consistently positive value. Moreover, it is important to note that the capacitor exhibits significant capacitance, allowing the output voltage to be rigorously maintained at the specified voltage "Vo.". It is assumed throughout this analysis that the components involved are ideal. The analysis unfolds through a systematic investigation of both inductor voltage and current under two distinct scenarios: when the switch is closed and when it is open [35][36].

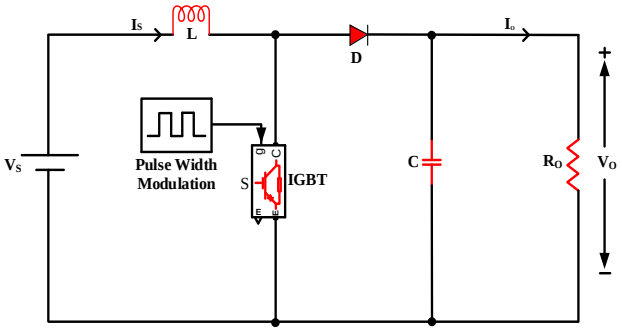

Figure (1): Boost (Step-Up) Converter Circuit.

These ripples are negligible when the switching action occurs at high frequencies. The circuit's operation can be categorized into two distinct modes: Mode 1 initiates when the switch is in the closed position, while Mode 2 begins when the switch is open. For the purposes of this study, a IGBT is employed to facilitate the switching process within the Boost circuit. Mode 1, illustrated in Figure 2, initiates when the switch is in the "on" position. During this phase, the current flows from the DC source to the inductor L and the switch, with the diode in a reverse-biased state, effectively blocking the current path to the load. The inductor current and the energy stored within it continue to increase until the switch is subsequently turned off [37][38].

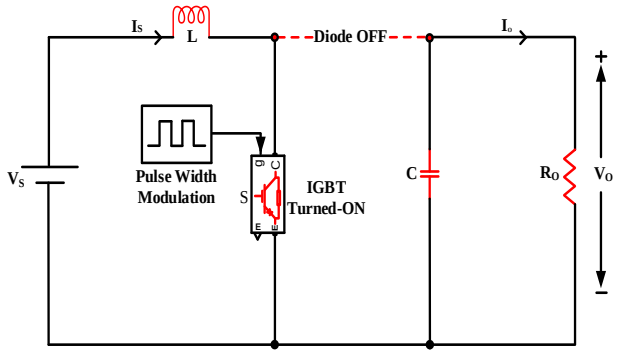

Figure (2): Boost (Step-Up) Converter Circuit ON State

ISSN: 2710-2165

$$V_L = V_S = L\frac{di_L}{d_t} \tag{1}$$

or

$$\frac{di_L}{d_t} = \frac{V_S}{L} \tag{2}$$

The current experiences a constant rate of change, resulting in a linear increase while the switch is in the closed position, as visually represented in Figure 3b. The alteration in inductor current is derived from this behavior [39][40].

$$\frac{\Delta i_L}{\Delta t} = \frac{\Delta i_L}{DT} = \frac{V_S}{L} \tag{3}$$

Therefore, the period during which this process occurs is referred to as the "on-time," denoted as t_{ON} = DT. The alteration in inductor current when the switch is closed can be calculated from the following equation:

$$\Delta i_{L_{ON}} = \frac{V_S DT}{L} \tag{4}$$

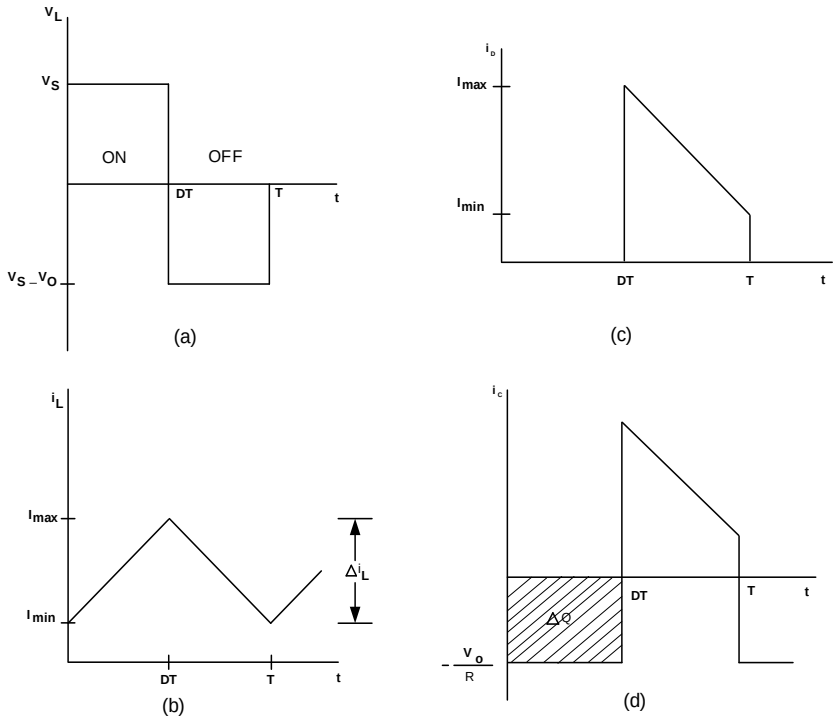

Figure (3) illustrates waveforms for a Boost converter, depicting various parameters: (a) Inductor voltage, (b) Inductor current, (c) Diode current, and (d) Capacitor current

Mode 2 commences when the switch is in the off state, as depicted in Figure 1(b). During this phase, the current that previously flowed through the inductor, capacitor, resistor load, and diode is affected. The inductor current diminishes until the switch is once again activated in the subsequent cycle, facilitating the transfer of the stored energy in the inductor to the load [41][42].

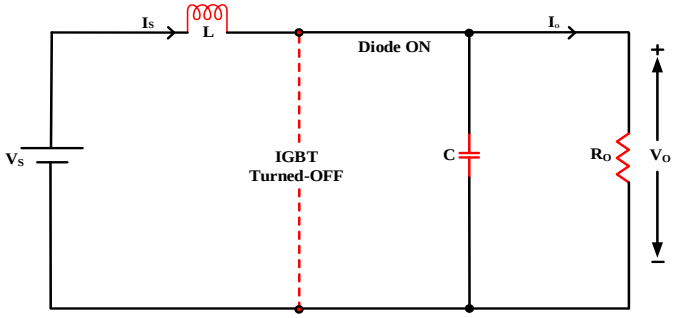

Figure (4): Boost (Step-Up) Converter Circuit OFF State

Under the assumption of a constant output voltage, denoted as "Vo", the voltage across the inductor is as follows.

$$V_L = V_S - V_O = L\frac{di_L}{d_t} \tag{5}$$

$$\frac{di_L}{d_t} = \frac{V_S - V_O}{L} \tag{6}$$

The inductor current experiences a consistent rate of change, necessitating a linear variation during the switch's open state. The alteration in inductor current while the switch remains open is as follows.

$$\frac{\Delta i_L}{\Delta t} = \frac{\Delta i_L}{(1-D)T} = \frac{V_S - V_O}{L} \tag{7}$$

In this state, the off-time duration is denoted as t_{oFF} = (1 - D) T. Consequently, the variation in inductor current can be calculated as follows:

$$\Delta i_{L_{OFF}} = \frac{(V_S - V_O)\,(1-D)T}{L} \tag{8}$$

By employing equations 4 and 8, the output voltage of the load V_L can be expressed as $\Delta i_{L_{ON}} + \Delta i_{L_{OFF}} = 0$.

$$\frac{V_S DT}{L} + \frac{(V_S - V_O)\,(1-D)T}{L} \tag{9}$$

Solving for Vo,

$$V_S(D + 1 - D) - V_O(1-D) = 0 \tag{10}$$

$$V_O = \frac{V_S}{1-D} \tag{11}$$

To ensure periodic operation, it is essential that the mean inductor voltage remains at zero. Expressing the average inductor voltage throughout one complete switching period and the solution for Vo produces an outcome identical to that obtained in Equation (11), we find that:

$$V_L = V_S D + (V_S - V_O)(1-D) = 0 \tag{12}$$

Equation (11), demonstrates that when the switch remains in the open state continuously with a duty cycle of D equal to zero, the output voltage aligns with the input voltage. As the duty ratio increases, the denominator within Equation (11) decreases, thereby leading to a higher output voltage.

The boost converter generates an output voltage that is either greater than or equal to the input voltage. Unlike the buck converter, the boost converter does not allow for an output voltage lower than the input voltage. When the duty ratio of the switch converges toward 1, the output voltage, as per Equation (11), tends towards infinity. It's worth noting, though, that Equation (11) is founded on the assumption of ideal components.

Actual components, characterized by inherent losses, will serve as a safeguard against such an eventuality. Figure 3, meanwhile, offers a graphical depiction of the voltage and current waveforms associated with the boost converter. The calculation of the average current in the inductor entails acknowledging the equivalence of the average power delivered by the source to the average power consumed by the load resistor. The output power can be defined as follows [43][44].

$$P_O = \frac{{V_O}^2}{R_O} = V_O I_O \tag{13}$$

The equation for input power is expressed as $V_S I_S = V_S I_L$. By equating input and output powers and utilizing the equation specified in (11).

$$V_S I_L = \frac{{V_O}^2}{R_O} = \frac{[V_S/(1-D)]^2}{R_O} = \frac{{V_S}^2}{(1-D)^2 R_O} \tag{14}$$

Through the process of solving for the average inductor current and incorporating several substitutions, it is possible to express I_L as follows:

$$I_L = \frac{V_S}{(1-D)^2 R_O} = \frac{{V_O}^2}{V_S R_O} = \frac{V_O I_O}{V_S} \tag{15}$$

The determination of maximum and minimum inductor currents relies on utilizing the average value and the current variation derived from Equation (4).

$$I_{max} = I_L + \frac{\Delta i_L}{2} = \frac{V_S}{(1-D)^2 R_O} + \frac{V_S DT}{2L} \tag{16}$$

$$I_{min} = I_L - \frac{\Delta i_L}{2} = \frac{V_S}{(1-D)^2 R_O} - \frac{V_S DT}{2L} \tag{17}$$

Equation (11) was formulated under the assumption that the inductor current remains continuous, signifying a constant positive flow. A prerequisite for achieving continuous inductor current is that $I_{\min}$ must be positive. Consequently, the demarcation point between continuous and discontinuous inductor current is established from Equation (18).

$$I_{min} = 0 = \frac{V_S}{(1-D)^2 R_O} - \frac{V_S DT}{2L} \tag{18}$$

or

$$\frac{V_S}{(1-D)^2 R_O} = \frac{V_S DT}{2L} = \frac{V_S D}{2Lf} \tag{19}$$

Thus, the essential combination of inductance and switching frequency necessary to sustain continuous current in the boost converter can be described as follows:

$$(Lf)_{min} = \frac{D(1-D)^2 R_O}{2} \tag{20}$$

or

$$L_{min} = \frac{D(1-D)^2 R_O}{2f} \tag{21}$$

A boost converter engineered for continuous-current operation will feature an inductor value exceeding the minimum threshold, L_{min}. From a design point of view, it proves beneficial to represent inductance, L, in relation to a desired current, denoted as Δi_L.

$$L = \frac{V_S DT}{\Delta i_L} = \frac{V_S D}{\Delta i_L f} \tag{22}$$

The calculation of the peak-to-peak output voltage ripple is achievable by examining the capacitor current waveform, as illustrated in Figure 3d. Furthermore, the alteration in capacitor charge can be determined by:

$$|\Delta Q| = \left(\frac{V_O}{R_O}\right) DT = C\Delta V_O \tag{23}$$

An equation describing the ripple voltage is as follows:

$$\Delta V_O = \frac{V_O DT}{R_O C} = \frac{V_O D}{R_O C f} \tag{24}$$

or

$$= \frac{\Delta V_O}{V_O} = \frac{D}{R_O C f} \tag{25}$$

When considering the switching frequency, denoted as f an alternative approach involves expressing capacitance in relation to the output voltage ripple, resulting in:

$$C = \frac{D}{R_O(\Delta V_O / V_O) f} \tag{26}$$

III. DESIGN BOOST (STEP-UP) CONVERTER

In this research, it is imperative to account for the peak-to-peak inductor current and the output voltage ripple when designing the boost converter circuit. The initial phase of the design process involves calculating the parameters of the boost converter circuit for two distinct input voltages, namely 10 V_{DC} and 20 V_{DC}. Once the values of the inductor (L) and capacitor (C) have been determined, the circuit is then modeled using MATLAB Simulink software, as depicted in Figures 5 and 6. Subsequently, the analysis includes a comparison between the calculated values and the simulation results.

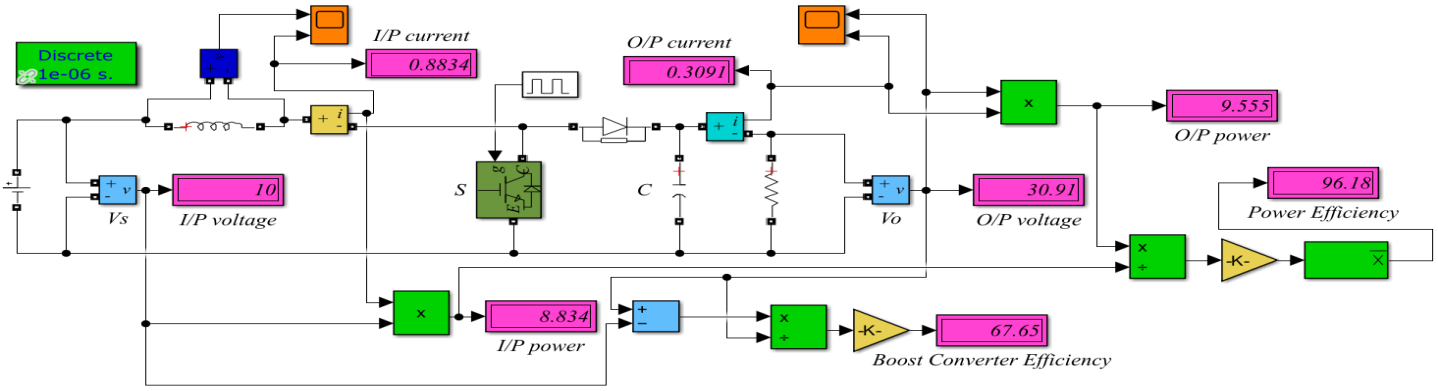

Figure (5): Boost (Step-Up) Converter at $V_S = 10$ Using MATLAB/Simulink

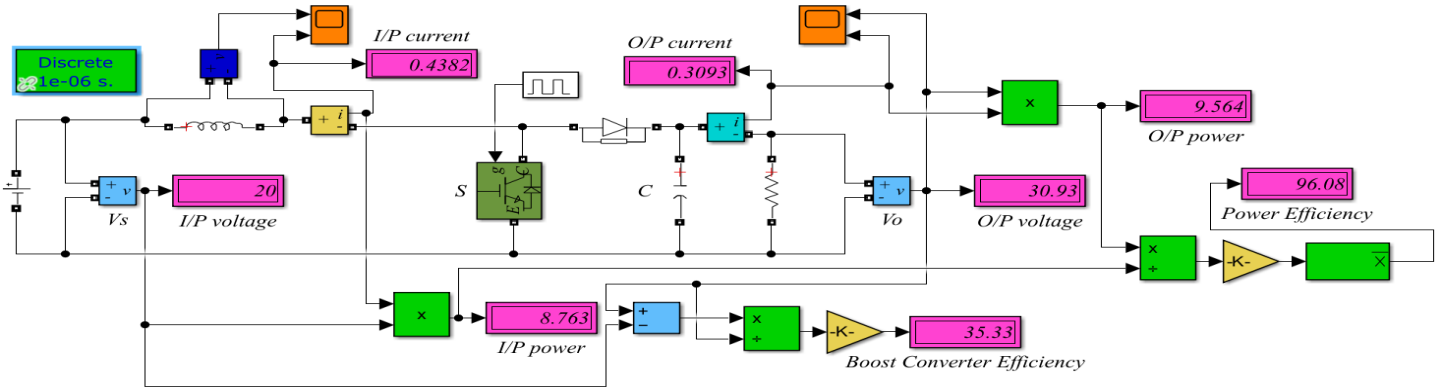

Figure (6): Boost (Step-Up) Converter at $V_S = 20$ Using MATLAB/Simulink

This analysis maintains a limit of a ripple inductor current, which should not exceed 25% of the total inductor current, and ensures that the output voltage ripple remains below 1%. The initial steps in designing Boost circuits, using a switching frequency value of 25 kHz as indicated in Table 1, are demonstrated in the calculations below:

Table (1): Boost (Step-up) Converter Calculations

Input voltage is 10 V_{DC} and output voltage is 30 V_{DC} and switching frequency value is 25 kHZ	Input voltage is 20 V_{DC} and output voltage is 30 V_{DC} and switching frequency value is 25 kHZ
$V_{LON} = V_S = 10$ V	$V_{LON} = V_S = 20$ V
$V_{LOFF} = V_S - V_O$=10-30 = -20 V	$V_{LOFF} = V_S - V_O$= 20-30 = -10 V
$D = 1 - \frac{V_S}{V_O}$ = 1-10/30 = 0.666	$D = 1 - \frac{V_S}{V_O}$ = 1-20/30 = 0.333
$L_{min} = \frac{D(1-D)^2 \cdot R_O}{2f} = \frac{0.666(1-0.666)^2 \cdot 100}{2 \cdot 25000} = 148.6\ \mu H$	$L_{min} = \frac{D(1-D)^2 \cdot R_O}{2f} = \frac{0.333(1-0.333)^2 \cdot 100}{2 \cdot 25000} = 296.3\ \mu H$
$I_L = \frac{V_S}{(1-D)^2 \cdot R_O} = \frac{10}{(1-0.666)^2 \times 100}$ =0.896	$I_L = \frac{V_S}{(1-D)^2 \cdot R_O} = \frac{20}{(1-0.333)^2 \times 100}$ =0.449
$\Delta i_L = \frac{25}{100} \cdot 0.896 = 0.224$	$\Delta i_L = \frac{25}{100} \cdot 0.449 = 0.112$
$L = \frac{V_S D}{\Delta i_L f} = \frac{10 \cdot 0.666}{0.224 \cdot 25000} = 1.189\ mH$	$L = \frac{V_S D}{\Delta i_L f} = \frac{20 \cdot 0.333}{0.112 \cdot 25000} = 2.378\ mH$

$I_{max} = I_L + \frac{\Delta iL}{2} = 0.896 + \frac{0.224}{2} = 1.008$	$I_{max} = I_L + \frac{\Delta iL}{2} = 0.449 + \frac{0.112}{2} = 0.505$
$I_{min} = I_L - \frac{\Delta iL}{2} = 0.896 - \frac{0.216}{2} = 0.788$	$I_{min} = I_L - \frac{\Delta iL}{2} = 0.449 - 0.112/2 = 0.393$
$I_O = \frac{V_O}{R_O} = \frac{30}{100} = 0.3\ A$	$I_O = \frac{V_O}{R_O} = \frac{30}{100} = 0.3\ A$
$C = \frac{D}{R_O \cdot (\Delta V_L/V_L) f} = \frac{0.666}{100 \cdot 0.01 \cdot 25000} = 26.64\ \mu F$	$C = \frac{D}{R_O \cdot (\Delta V_L/V_L) f} = \frac{0.333}{100 \cdot 0.01 \cdot 25000} = 13.32\ \mu F$
Boost Converter Efficiency, E_{boost} $E_{boost} = \frac{(V_O - V_S)}{V_O} \cdot 100\% = \frac{(30\_10)}{30} \cdot 100\% = 66.33\%$	Boost Converter Efficiency, E_{boost} $E_{boost} = \frac{(30\_20)}{30} \cdot 100\% = \frac{(30\_20)}{30} \cdot 100\% = 33.33\%$
$P_S = V_S \cdot I_L = 10 \cdot 0.896 = 8.96$ W	$P_S = V_S \cdot I_L = 20 \cdot 0.449 = 8.98$ W
$P_O = V_O \cdot I_O = 30 \cdot 0.3 = 9$ W	$P_O = V_O \cdot I_O = 30 \cdot 0.3 = 9$ W
Power Efficiency, η $\eta = \frac{P_O}{P_i} \cdot 100\% = \frac{9}{8.96} \cdot 100\% = 100.45\%$	Power Efficiency, η $\eta = \frac{P_O}{P_i} \cdot 100\% = \frac{9}{8.98} \cdot 100\% = 100.22\%$

IV. Simulation Results

In the initial stage, a boost converter is engineered, employing IGBT technology, featuring a switching frequency of 25 kHz, an input voltage of 10 V_{DC}, and a duty cycle set at 0.66. Following the calculations, the inductor's value is determined to be 1.189 mH, and the capacitor's value is measured at 26.64 µF. The circuit design and results are obtained using MATLAB Simulink.

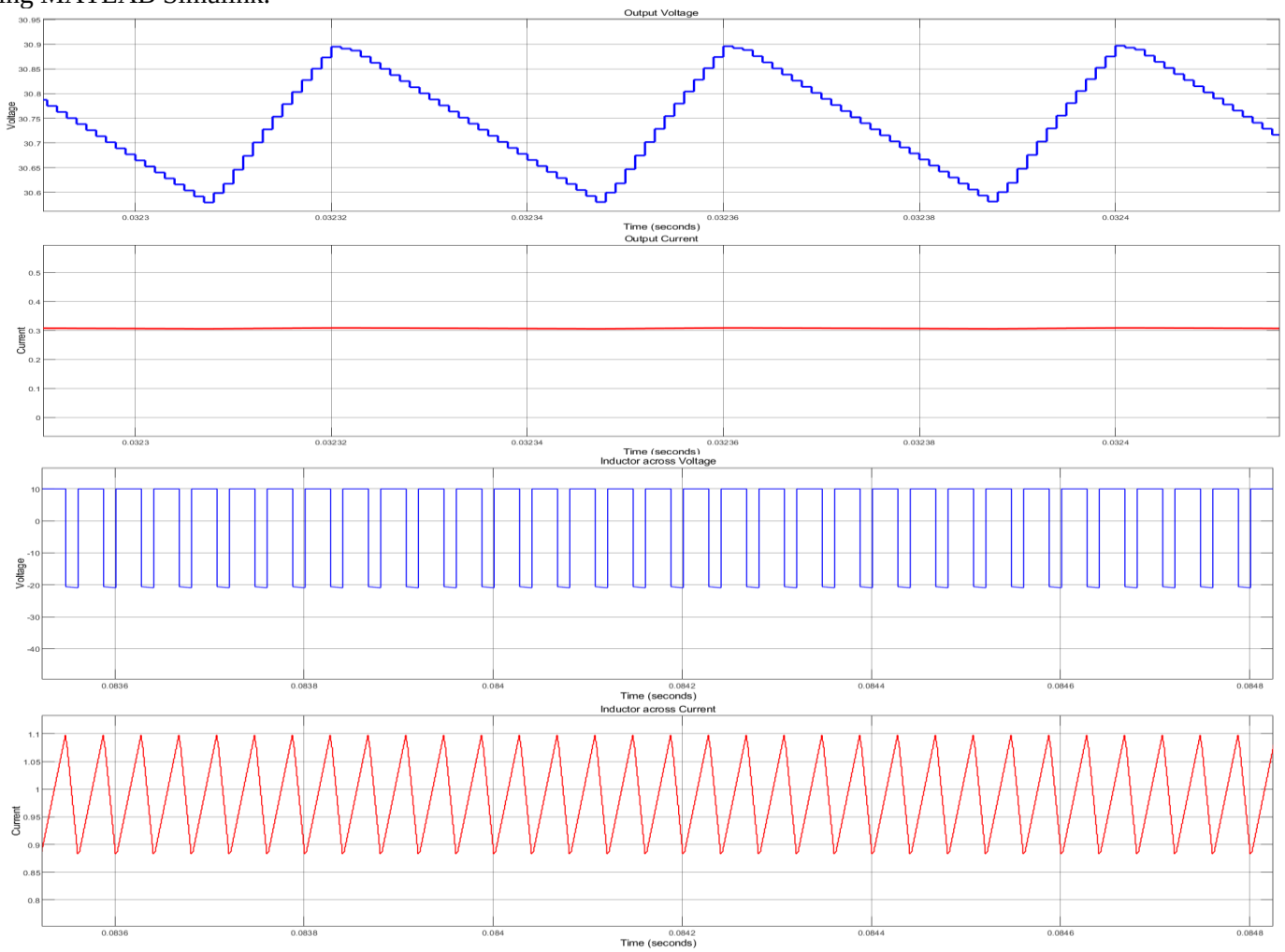

Figure (7): Boost converter waveform for output voltage, output current, Inductor voltage and Inductor current

Referring to Table 2, both the theoretical and simulated outcomes of the boost converter circuit design exhibit a close alignment, demonstrating the accuracy of the design in Table 1. Consequently, the simulation results significantly influence the selection of appropriate inductor and capacitor values. Conversely, as the duty cycle increases, there is a noticeable reduction in ripple current and associated losses.

Table (2): A Comparative Analysis of Parameters Between Theoretical Calculation and Simulation Results

Parameters	Calculation	Simulation	Relative Error	Accuracy
VL_{ON}	10 V	10 V	0.000	1
VL_{OFF}	-20 V	-20.12 V	0.006	0.994
I_L	0.896 A	0.8834 A	0.014	0.986
ΔiL	0.224 A	0.22 A	0.018	0.982
I_{max}	1.008 A	1.1 A	0.004	0.996
I_{min}	0.788 A	0.81 A	0.027	0.973
V_O	30 V	30.91 V	0.029	0.971
$\Delta V_L/V_L$	0.01	0.01	0.000	1
E_{boost}	66.33	67.65	0.019	0.981
η	100.45	96.18	0.044	0.956

In the subsequent analysis, the boost converter was designed with characteristic input parameters a voltage of 20 V_{DC} and a duty cycle of 0.33. According to the calculations, the inductance is computed as 2.378 mH, and the capacitance is determined to be 13.32 µF.

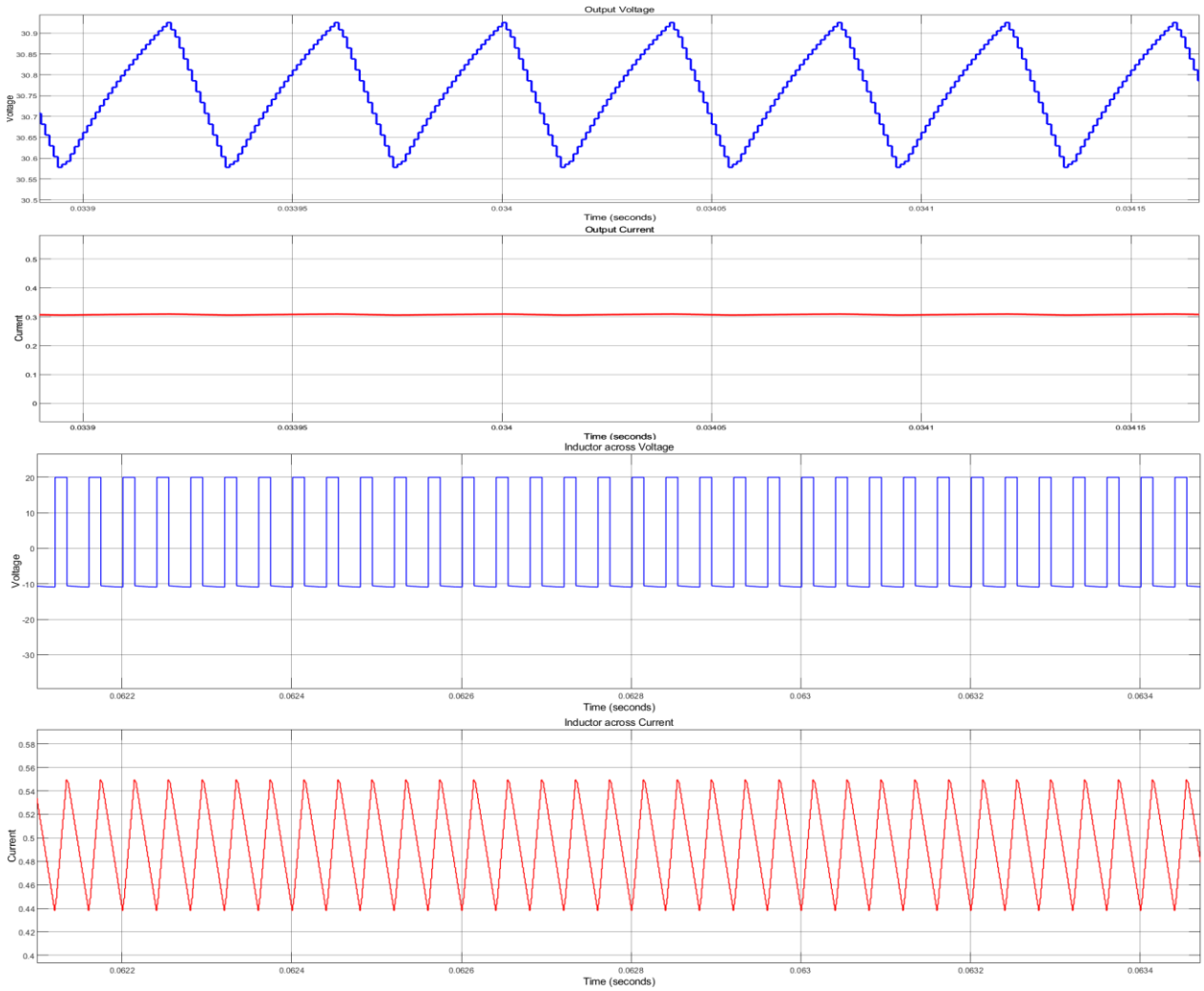

Figure (8): Boost converter waveform for output voltage, output current, Inductor voltage and Inductor current

Table 3: A Comparative Analysis of Parameters Between Theoretical Calculation and Simulation Results

Parameters	Calculation	Simulation	Relative Error	Accuracy
VL_{ON}	20 V	10.12 V	0.000	1
VL_{OFF}	-10 V	-10.12 V	0.012	0.988
I_L	0.449A	0.438 A	0.025	0.975
ΔiL	0.112 A	0.107 A	0.046	0.954
I_{max}	0.505 A	0.509 A	0.0078	0.992
I_{min}	0.393 A	0.396 A	0.076	0.925
V_O	30 V	30.93 V	0.030	0.97
$\Delta V_L/V_L$	0.01	0.01	0.000	1
E_{boost}	33.33	35.33	0.056	0.944
η	100.22	96.08	0.043	0.957

When reviewing the results presented in Table 3, it is clear that the accuracy remains close to unity (1). This indicates that even when a different input source is used compared to the previous design, accuracy can be maintained, provided the appropriate inductor and capacitor values are carefully chosen.

V. CONCLUSION

In the context of the boost converter circuit design step by step, parameters such as the input switching frequency, the percentage of ripple in the inductor current relative to its average value, and the output voltage ripple can collectively serve as indicators for deducing the appropriate values for both the capacitor and the inductor. A comparative analysis was conducted between the simulation and theoretical outcomes, focusing on the appropriateness of the selected values for the inductor and capacitor. The results indicate that even with variations in the input supply, the output voltage can be sustained when the design parameters are taken into account. Notably, both circuits exhibit an accuracy closely approximating unity, signifying the successful design and development of both systems. The design assessment of this circuit seeks to stabilize the output voltage at 30 VDC by regulating the input voltage. Theoretical and simulation results indicate power conversion efficiencies of 100.45% and 96.18%, respectively, for an input voltage of 10V, while for an input voltage of 20V, the corresponding efficiencies are 100.22% and 96.08%, respectively.

ACKNOWLEDGMENT

The authors would like to thank the College of Engineering, Al-Iraqia University.

REFERENCES

[1] T. Sutikno, A. S. Samosir, R. A. Aprilianto, H. S. Purnama, W. Arsadiando, and S. Padmanaban, "Advanced DC-DC converter topologies for solar energy harvesting applications: A review," *Clean Energy*, vol. 7, no. 3, pp. 555–570, 2023, doi: 10.1093/ce/zkad003.

[2] S. A. Lopa, S. Hossain, M. K. Hasan, and T. K. Chakraborty, "Design and Simulation of DC-DC Converters," *Int. Res. J. Eng. Technol.*, pp. 2395–56, 2016.

[3] J. J.Duair, A. I. Majeed, and G. M. Ali, "Design of Maximum Power Point Tracker Controller for Boost Converter Photovoltaic Array System Based on Fuzzy Mamdani Logic," *J. Eng. Sustain. Dev.*, vol. 25, no. Special, pp. 1-13-1–25, 2021, doi: 10.31272/jeasd.conf.2.1.3.

[4] M. M. S. Sulong *et al.*, "Design and Simulation of High Gain DC-DC Boost Converter System for PV Application," *4th Int. Iraqi Conf. Eng. Technol. Their Appl. IICETA 2021*, no. October 2022, pp. 179–183, 2021, doi: 10.1109/IICETA51758.2021.9717915.

[5] V. Behravesh, R. Keypour, and A. Akbari Foroud, "Control strategy for improving voltage quality in residential power distribution network consisting of roof-top photovoltaic-wind hybrid systems, battery storage and electric vehicles," *Sol. Energy*, vol. 182, no. February, pp. 80–95, 2019, doi: 10.1016/j.solener.2019.02.037.

[6] M. Ben Ammar, S. Sahnoun, A. Fakhfakh, and O. Kanoun, "Design of a DC-DC Boost Converter of Hybrid Energy Harvester for Low-Power Biomedical Applications," *Proc. 17th Int. Multi-Conference Syst. Signals Devices, SSD 2020*, pp. 955–959, 2020, doi: 10.1109/SSD49366.2020.9364118.

[7] M. P. State, "Analysis , Design and Modeling of Dc-Dc Converter Using Analysis , Design and Modeling of Dc-Dc Converter Using Simulink," 2004.

[8] M. Dursun and A. Gorgun, "Analysis and performance comparison of DC-DC power converters used in photovoltaic systems," *2017 4th Int. Conf. Electr. Electron. Eng. ICEEE 2017*, pp. 113–119, 2017, doi: 10.1109/ICEEE2.2017.7935804.

[9] S. Sivakumar, M. J. Sathik, P. S. Manoj, and G. Sundararajan, "An assessment on performance of DC-DC converters for renewable energy applications," *Renew. Sustain. Energy Rev.*, vol. 58, pp. 1475–1485, 2016, doi: 10.1016/j.rser.2015.12.057.

[10] R. Ayop and C. W. Tan, "Design of boost converter based on maximum power point resistance for photovoltaic applications," *Sol. Energy*, vol. 160, no. August 2017, pp. 322–335, 2018, doi: 10.1016/j.solener.2017.12.016.
[11] M. L. Katche, A. B. Makokha, S. O. Zachary, and M. S. Adaramola, "A Comprehensive Review of Maximum Power Point Tracking (MPPT) Techniques Used in Solar PV Systems," *Energies*, vol. 16, no. 5, 2023, doi: 10.3390/en16052206.
[12] A. S. Mansour, E. M. Sarhan, A. E. El-sabbe, and D. S. M. Osheba, "A Single-switch Non-isolated High Gain DC / DC Converter for PV Applications Electrical Engineering Department , Faculty of Engineering , Menoufia University , Shebin El-Kom Master of Science Candidate," vol. 45, no. 3, pp. 261–271, 2022.
[13] L. Zaghba, A. Borni, A. Bouchakour, and N. Terki, "Buck-boost converter system modelling and incremental inductance algorithm for photovoltaic system via Matlab / Simulink," *evue des Energies Renouvelables SIENR'14 Ghardaïa*, pp. 63–70, 2014.
[14] D. Bui, T. M. Mostafa, A. P. Hu, and R. Hattori, "DC-DC Converter Based Impedance Matching for Maximum Power Transfer of CPT System with High Efficiency," *2018 IEEE PELS Work. Emerg. Technol. Wirel. Power Transf. Wow 2018*, no. May 2019, pp. 1–5, 2018, doi: 10.1109/WoW.2018.8450929.
[15] R. Reshma Gopi and S. Sreejith, "Converter topologies in photovoltaic applications – A review," *Renew. Sustain. Energy Rev.*, vol. 94, no. December 2017, pp. 1–14, 2018, doi: 10.1016/j.rser.2018.05.047.
[16] K. S. Jyothi, "Battery Charging from Solar using Buck Converter with MPPT," *Int. J. Res. Appl. Sci. Eng. Technol.*, vol. 9, no. VI, pp. 3490–3493, 2021, doi: 10.22214/ijraset.2021.35919.
[17] J. Veerabhadra and S. Nagaraja Rao, "Comparative assessment of high gain boost converters for renewable energy sources and electrical vehicle applications," *Energy Harvest. Syst.*, no. March, 2023, doi: 10.1515/ehs-2022-0144.
[18] A. A. Lund, "Boost converter design with feedback control Boost converter design with feedback control," 2021.
[19] A. Charaabi, O. Barambones, A. Zaidi, and N. Zanzouri, "A novel two stage controller for a dc-dc boost converter to harvest maximum energy from the PV power generation," *Actuators*, vol. 9, no. 2, 2020, doi: 10.3390/ACT9020029.
[20] H. Hussein, A. Mahdi, and T. Abdul-Wahhab, "Design of a Boost Converter with MPPT Algorithm for a PV Generator Under Extreme Operating Conditions," *Eng. Technol. J.*, vol. 39, no. 10, pp. 1473–1480, 2021, doi: 10.30684/etj.v39i10.1888.
[21] M. H. Taghvaee, M. A. M. Radzi, S. M. Moosavain, H. Hizam, and M. Hamiruce Marhaban, "A current and future study on non-isolated DC-DC converters for photovoltaic applications," *Renew. Sustain. Energy Rev.*, vol. 17, no. January, pp. 216–227, 2013, doi: 10.1016/j.rser.2012.09.023.
[22] J. Gnanavadivel, K. Jayanthi, S. Vasundhara, K. V. Swetha, and K. Jeya Keerthana, "Analysis and design of high gain DC-DC converter for renewable energy applications," *Automatika*, vol. 64, no. 3, pp. 408–421, 2023, doi: 10.1080/00051144.2023.2170062.
[23] K. B. Nandha, K. Reddy, N. A. Kumar, K. Karthik, P. N. Kumar, and T. S. Deepak, "' Study of DC-DC Converters in PV Systems using MPPT Algorithm ,'" no. 7, pp. 402–407, 2023, doi: 10.46647/ijetms.2023.v07si01.067.
[24] J. López Seguel, S. I. Seleme, and L. M. F. Morais, "Comparison of the performance of mppt methods applied in converters buck and buck-boost for autonomous photovoltaic systems," *Ingeniare*, vol. 29, no. 2, pp. 229–244, 2021, doi: 10.4067/S0718-33052021000200229.
[25] A. Agrahari, A. Verma, A. Maurya, and A. K. Pandey, "Comparative Analysis of Various DC-DC Converters using MATLAB," vol. 11, no. 04, pp. 190–200, 2022, [Online]. Available: www.ijert.org
[26] S. P. Litrán, E. Durán, J. Semião, and R. S. Barroso, "Single-switch bipolar output dc-dc converter for photovoltaic application," *Electron.*, vol. 9, no. 7, pp. 1–14, 2020, doi: 10.3390/electronics9071171.
[27] R. F. Coelho, W. M. Dos Santos, and D. C. Martins, "Influence of power converters on PV maximum power point tracking efficiency," *2012 10th IEEE/IAS Int. Conf. Ind. Appl. INDUSCON 2012*, no. February, 2012, doi: 10.1109/INDUSCON.2012.6453083.
[28] P. Rajivgandhi, S. A. Elankurisil, and M. Dinesh, "Improved Efficiency of the Solar Energy in Photovoltaic Systems with Direct Control Method Using SEPIC Converter," vol. 5, no. 5, pp. 100–108, 2020.
[29] S. Senthilkumar, V. Mohan, S. P. Mangaiyarkarasi, and M. Karthikeyan, "Analysis of Single-Diode PV Model and Optimized MPPT Model for Different Environmental Conditions," *Int. Trans. Electr. Energy Syst.*, vol. 2022, 2022, doi: 10.1155/2022/4980843.
[30] C. S. Lee, S. S. Kim, and J. H. Yu, "Load and frequency dependent CMOS dual-mode DC-DC converter," *Microelectronics J.*, vol. 92, no. September, p. 104610, 2019, doi: 10.1016/j.mejo.2019.104610.
[31] I. Ait Ayad, E. Elwarraki, and M. Baghdadi, "Intelligent Perturb and Observe Based MPPT Approach Using Multilevel DC-DC Converter to Improve PV Production System," *J. Electr. Comput. Eng.*, vol. 2021, no. Ic, 2021, doi: 10.1155/2021/6673022.
[32] A. Raj and R. P. Praveen, "Highly efficient DC-DC boost converter implemented with improved MPPT algorithm for utility level photovoltaic applications," *Ain Shams Eng. J.*, vol. 13, no. 3, p. 101617, 2022, doi: 10.1016/j.asej.2021.10.012.
[33] T. W. Hariyadi and A. Adriansyah, "Comparison of DC-DC Converters Boost Type in Optimizing the Use of Solar Panels," *2020 2nd Int. Conf. Broadband Commun. Wirel. Sensors Powering, BCWSP 2020*, pp. 189–194, 2020, doi: 10.1109/BCWSP50066.2020.9249464.
[34] J. F. J. Van Rensburg, M. J. Case, and D. V. Nicolae, "Double-boost DC to DC converter," *IECON Proc. (Industrial Electron. Conf.*, no. 0, pp. 707–711, 2008, doi: 10.1109/IECON.2008.4758040.

[35] A. Pradhan and B. Panda, "A simplified design and modeling of boost converter for photovoltaic sytem," *Int. J. Electr. Comput. Eng.*, vol. 8, no. 1, pp. 141–149, 2018, doi: 10.11591/ijece.v8i1.pp141-149.
[36] A. Thiyagarajan, S. G. Praveen Kumar, and A. Nandini, "Analysis and comparison of conventional and interleaved DC/DC boost converter," *2nd Int. Conf. Curr. Trends Eng. Technol. ICCTET 2014*, vol. 38, no. 0, pp. 198–205, 2014, doi: 10.1109/ICCTET.2014.6966287.
[37] R. Y. Barazarte, "Design of a Two-Level Boost Converter," pp. 1–10, 2013.
[38] J. Chauhan, P. Chauhan, T. Maniar, and A. Joshi, "Comparison of MPPT algorithms for DC-DC converters based photovoltaic systems," *2013 Int. Conf. Energy Effic. Technol. Sustain. ICEETS 2013*, vol. 1, no. 1, pp. 476–481, 2013, doi: 10.1109/ICEETS.2013.6533431.
[39] D. Verma, S. Nema, R. Agrawal, Y. Sawle, and A. Kumar, "A Different Approach for Maximum Power Point Tracking (MPPT) Using Impedance Matching through Non-Isolated DC-DC Converters in Solar Photovoltaic Systems," *Electron.*, vol. 11, no. 7, 2022, doi: 10.3390/electronics11071053.
[40] S. Kolsi, H. Samet, and M. Ben Amar, "Design Analysis of DC-DC Converters Connected to a Photovoltaic Generator and Controlled by MPPT for Optimal Energy Transfer throughout a Clear Day," *J. Power Energy Eng.*, vol. 02, no. 01, pp. 27–34, 2014, doi: 10.4236/jpee.2014.21004.
[41] N. Hashim, Z. Salam, D. Johari, and N. F. N. Ismail, "DC-DC boost converter design for fast and accurate MPPT algorithms in stand-alone photovoltaic system," *Int. J. Power Electron. Drive Syst.*, vol. 9, no. 3, pp. 1038–1050, 2018, doi: 10.11591/ijpeds.v9.i3.pp1038-1050.
[42] Z. Liu, J. Du, and B. Yu, "Design method of double-boost DC/DC converter with high voltage gain for electric vehicles," *World Electr. Veh. J.*, vol. 11, no. 4, pp. 1–21, 2020, doi: 10.3390/wevj11040064.
[43] L. S. Xavier, W. C. S. Amorim, A. F. Cupertino, V. F. Mendes, W. C. do Boaventura, and H. A. Pereira, "Power converters for battery energy storage systems connected to medium voltage systems: a comprehensive review," *BMC Energy*, vol. 1, no. 1, pp. 1–15, 2019, doi: 10.1186/s42500-019-0006-5.
[44] N. Abouchabana, M. Haddadi, A. Rabhi, A. D. Grasso, and G. M. Tina, "Power efficiency improvement of a boost converter using a coupled inductor with a fuzzy logic controller: Application to a photovoltaic system," *Appl. Sci.*, vol. 11, no. 3, pp. 1–19, 2021, doi: 10.3390/app11030980.